

Possibility of observable signatures of leptonium from astrophysical sources

S. C. Ellis*

*Australian Astronomical Observatory, 105 Delhi Road, North Ryde, New South Wales 2113, Australia
and Sydney Institute for Astronomy, School of Physics, University of Sydney,
New South Wales 2006, Australia*

Joss Bland-Hawthorn†

*Sydney Institute for Astronomy, School of Physics, University of Sydney, New South Wales 2006, Australia
(Received 27 January 2015; published 3 June 2015)*

The formation of positronium in our Galaxy is well measured, and has led to important and unanswered questions on the origin of the positrons. In principle it should be possible to form analogous systems from μ and τ leptons, viz. true muonium and true tauonium. However the probability of formation for these systems is greatly reduced due to the intrinsically short lifetimes of the μ and τ leptons. Likewise, the decay of the atoms is hastened by the high probability of the constituent particles decaying. Nevertheless, if sufficient numbers of μ and τ pairs are produced in high energy astrophysical environments there may be significant production of true muonium and true tauonium, despite the small probabilities. This paper addresses this possibility. We have calculated the pair production spectra of μ and τ leptons from photon-photon annihilation and electron-positron annihilation in astrophysical environments. We have computed the cross sections for radiative recombination and direct annihilation of the pairs, and the decay constants for the various allowable decays, and the wavelengths and energies of the recombination and annihilation signatures. In this way we have calculated the probabilities for the formation of true muonium and true tauonium, and the branching ratios for the various observable signatures. We have estimated the expected fluxes from accretion disks around microquasars and active galactic nuclei, and from interactions of jets with clouds and stars. We find that accretion disks around stellar mass black holes in our own Galaxy should have observable signatures at x-ray and γ -ray energies that are in principle observable with current observatories.

DOI: [10.1103/PhysRevD.91.123004](https://doi.org/10.1103/PhysRevD.91.123004)

PACS numbers: 34.80.Lx, 13.66.De, 36.10.Dr, 95.30.Cq

I. INTRODUCTION

In the years 1928–1931 Dirac introduced the concept of antimatter [1–3]. In 1932 Anderson showed that these theoretical concepts were real with the detection of the positron [4]. Then in 1934 Mohorovičić published a paper on the possibility of observing positronium (Ps) from astrophysical sources via its recombination lines [5]. This prescient paper went largely unnoticed, and the existence of Ps was predicted independently and separately by Pirenne [6], Ruark [7], Landau (unpublished work referred to in Alichanian and Asatiani [8]) and Wheeler [9].

To date, the observational challenge laid down by Mohorovičić, viz. to detect astrophysical sources of Ps from its recombination lines, has not been met. However the possibility of detection of Ps recombination lines has been raised on subsequent occasions inspired by advances in technology [10–12]. Despite the nondetection of Ps recombination lines, there is clear evidence of its existence in the Galaxy from its annihilation signature [13]; see the recent review by Prantzos *et al.* [14].

The observations of annihilating electrons and positrons in our Galaxy have raised several important questions for astrophysics, the foremost being, what are the sources of the positrons? Can they be explained with conventional astrophysics (e.g. high energy sources) or are more exotic sources required (e.g. annihilating dark matter)? Why is the annihilation radiation centered so strongly on the nucleus of the Galaxy with relatively little disk emission? How far do positrons disperse through the Galaxy before annihilation?

In this paper we address the question of what other observable signatures there are, arising from other leptonic atoms. For example, it is possible in principle to form atoms of $\mu^- - \mu^+$ and $\tau^- - \tau^+$. However, in these cases the observable signatures are complicated by the fact that the constituent particles are themselves unstable, and may decay prior to annihilation or transitions [15]. It is important to note that even improbable signatures may be significant if the rate of production of the atom is high enough; this situation is often very relevant in astrophysical situations. For example the hydrogen 21 cm emission line that results from the spin-flip transition between the hyperfine splitting of the 2S ground state has been hugely exploited in radio astronomy since the 1950s [16,17], although it has a transition probability of only $2.9 \times 10^{-15} \text{ s}^{-1}$.

*sellis@ao.gov.au

†jhb@physics.usyd.edu.au

Even faint signatures would be of interest. First, they would be the first such observations of $\mu^- - \mu^+$ or $\tau^- - \tau^+$, either in astrophysics or in the laboratory. Second, they would place constraints on the energetics and rate of production of μ or τ in astrophysical sources. Third, the rate of $\mu^- - \mu^+$ or $\tau^- - \tau^+$ production, compared with estimates of μ or τ production rates, would place constraints on the physical conditions during recombination.

Such measurements could be very useful. Taking the example of Ps, the rate, distribution and energetics of formation are all well measured, but the identity of positron sources still remains unclear. This is largely because it is difficult to reproduce the distribution of Ps emission, and also because there are many e^+ candidates, which are difficult to distinguish observationally. Observations, or even nondetection, of $\mu^- - \mu^+$ or $\tau^- - \tau^+$ could place further constraints on the competing models for the origin of Galactic positrons.

The study of such processes is important, even if they are unlikely. Anomalous spectral signatures are routinely discovered, for example the recent detection of an unidentified emission line in the x-ray spectra of clusters of galaxies at 3.5 keV [18,19]. We note that this line is not attributable to $\mu^- - \mu^+$ or $\tau^- - \tau^+$, although these species are expected to produce x-ray emission lines, as we show. Nevertheless, in such cases it is important to rule out prosaic, but poorly understood processes before accepting more exotic physics. The formation of $\mu^- - \mu^+$ and $\tau^- - \tau^+$ in astrophysical environments has so far received very little attention, but should not be rejected *a priori* on the basis of the short lifetimes of the μ and τ .

The production of $\mu^- - \mu^+$ and $\tau^- - \tau^+$ in electron-positron colliders is difficult due to the rapid decay times of the particles, although methods have been proposed for the creation of $\mu^- - \mu^+$ [20]. It may be possible to bypass these difficulties if large numbers of leptonium atoms are produced in high energy astrophysical environments. This is an important possibility since neither $\mu^- - \mu^+$ nor $\tau^- - \tau^+$ have ever been observed, and together they are the most compact pure QED systems that could exist. An astrophysical detection would be more difficult to interpret than a collider detection, but would nevertheless constitute an important basic test of QED.

We wish to make a first step in addressing this challenge by calculating the expected observable signatures of astrophysical sources. Consider a source of particle-antiparticle lepton pairs. Their possible fates are (i) the particle immediately decays, if it is μ^\pm or τ^\pm , (ii) it directly annihilates with its antiparticle, (iii) it radiatively recombines with a free particle, then annihilates, (iv) it forms a new atom via charge exchange, then annihilates.

Ps clearly has the highest probability of forming, since its constituent particles are stable, and can travel through the interstellar medium until they form Ps through charge exchange or radiative recombination, although they may

also directly annihilate in flight or when thermalized. The probabilities for Ps formation have been discussed in detail [10,21,22], and Ps formation at the Galactic center is confirmed by the observation of the 511 keV annihilation signature and the three photon triplet annihilation continuum [23], from which a Ps formation fraction of ≈ 97 percent is inferred. See Prantzos *et al.* [14] for a recent review of Ps astrophysics.

The formation of any atom having a μ or τ lepton is much less likely, since the decay times are so short that no travel of the particles is possible. Thus, we only consider the formation of true muonium and true tauonium (hereafter referred to as M and T [24]) *in situ*, i.e., the particle-antiparticle pairs must be created with an energy less than the ionization energy, so that the particle forms immediately. A summary of the basic properties of M, T and Ps, to which frequent comparisons are made, is given in Table I; the calculations or references for these values can be found throughout the paper, in the sections given in the final column of the table.

To calculate the likelihood of forming M and T, we begin by reviewing the possible mechanisms for pair production which are relevant in astrophysical environments (Sec. II). We then use the relevant cross sections for pair production, to calculate the pair-production spectra, and from these calculate the fraction of pairs which have sufficiently low energy to form an onium immediately, i.e., the fraction of pairs produced with kinetic energy less than the ionization energy of the atom (Sec. III). These pairs may either directly annihilate or radiatively recombine, and we calculate the branching fraction for these processes in Sec. IV. For those that do radiatively recombine, we calculate the cross sections for radiative recombination, and hence the fractions which recombine into the nL th quantum level in Sec. IVA. Then in Sec. V we calculate the different decay channels and in Sec. VI the resulting branching ratios for an onium in the n th level, and thus the total branching fractions for specific observational signatures. The signatures themselves are discussed in Sec. VII. This brings us to a position where, for a given rate of pair production, we can estimate the luminosity of each of the different decay channels, and we apply these calculations to specific astrophysical sources in Sec. VIII. We give our conclusions in Sec. IX.

II. PAIR-PRODUCTION PROCESSES IN ASTROPHYSICAL ENVIRONMENTS

The formation of leptonium other than Ps is not complicated by possibilities of escape, in-flight formation, charge-exchange etc.; the lifetimes of the particles themselves are so short (Sec. V), that if an atom is not formed immediately after the creation of a particle, then the particle itself will decay before any of these processes can occur. Ultrarelativistic particles may live longer due to time

TABLE I. Summary of the main properties of Ps, M and T.

		Ps	M	T	Section
Rest mass/annihilation energy (MeV)		0.511	105.66	1406.6	
Ionization energy (eV)		6.8	1784.1	23751.4	Sec. II
Bohr radius (m)		1.058×10^{-10}	5.199×10^{-13}	3.044×10^{-14}	Sec. VC
Decay time of constituent particles (s)		∞	2.197×10^{-6}	2.874×10^{-13}	Sec. VB
$\gamma\gamma$ annihilation time (ground state) (s)	Singlet	1.2×10^{-10}	6.0×10^{-13}	3.6×10^{-14}	Sec. VA
	Triplet	1.4×10^{-7}	6.7×10^{-10}	4.0×10^{-11}	Sec. VA
e^-e^+ annihilation time (ground state) (s)	Triplet	\dots	1.8×10^{-12}	1.1×10^{-13}	Sec. VA
Recombination time ($nL \rightarrow n'L'$) (s)	$21 \rightarrow 10$ (Lyman α)	3.191×10^{-9}	1.543×10^{-11}	9.18×10^{-13}	Sec. VC
	$31 \rightarrow 10$ (Lyman β)	1.195×10^{-8}	5.780×10^{-11}	3.44×10^{-12}	Sec. VC
	$31 \rightarrow 20$	8.905×10^{-8}	4.307×10^{-10}	2.56×10^{-11}	Sec. VC
	$30 \rightarrow 21$	3.166×10^{-7}	1.531×10^{-9}	9.11×10^{-11}	Sec. VC
	$32 \rightarrow 21$	3.092×10^{-8}	1.495×10^{-10}	8.89×10^{-12}	Sec. VC
	$41 \rightarrow 20$	2.068×10^{-7}	9.999×10^{-10}	5.95×10^{-11}	Sec. VC
	$40 \rightarrow 21$	7.753×10^{-7}	3.750×10^{-9}	2.23×10^{-10}	Sec. VC
	$42 \rightarrow 21$	9.692×10^{-8}	4.687×10^{-10}	2.79×10^{-11}	Sec. VC
Recombination energies (keV)	Lyman α	5.102×10^{-3}	1.055	17.7	Sec. VC
	Lyman β	6.047×10^{-3}	1.250	21.0	Sec. VC
	Balmer α	9.448×10^{-4}	0.195	3.3	Sec. VC
	Balmer β	1.276×10^{-3}	0.264	4.4	Sec. VC

dilation, but as for e^+ [25], the annihilation signature will give rise to very weak continuum emission.

We consider the following production processes for leptons, l ,

$$\pi^- \rightarrow l^- + \bar{\nu}_l, \quad (1)$$

$$\pi^+ \rightarrow l^+ + \nu_l, \quad (2)$$

$$\gamma + \gamma \rightarrow l^- + l^+, \quad (3)$$

$$e^- + e^+ \rightarrow l^- + l^+. \quad (4)$$

The pion decay processes will occur in collisions of highly energetic (> 200 MeV) cosmic rays with protons in the interstellar medium (ISM) [26]. The third process requires very high photon energies and will occur in the high energy environments surrounding compact objects, such as black holes and neutron stars [26]. The last process may occur if the e^+ have large kinetic energy and collide with e^- in the ISM, e.g. if an e^\pm jet from an active galactic nucleus (AGN) or microquasar collides with an interstellar cloud of gas or a star.

We can immediately dismiss the pion decay processes as irrelevant for τ leptons, since the τ are more massive than the π^\pm . We can also dismiss the pion decay processes as irrelevant for the formation of M, on two grounds. First, only a single particle is produced, and the probability of radiative recombination with another free μ before it decays is negligible. Second, the energetics are unfavorable. Since the reaction involves a single particle of known mass

decaying into two particles, the energetics are precisely determined in the zero-momentum frame; the μ is created with a kinetic energy of 4.12 MeV, which is much higher than the ionization energy of M, ≈ 1.4 keV. Thus the created μ must first lose energy, then collide with its antiparticle, before either particle decays, the probability of which is negligible.

This leaves us with photon-photon pair production and electron-positron pair production. In both these processes the μ (or τ) will be created with typical energies much higher than the ionization energy of M (or T) (≈ 1.4 keV for M, and ≈ 23.7 keV for T). Only the small fraction of pairs whose total kinetic energy in the zero-momentum (z.m.) frame is less than the ionization energy can form an onium, i.e.,

$$T_1 + T_2 \leq E_{\text{ion}}, \quad (5)$$

$$2(\gamma - 1)mc^2 \leq \frac{\mu q^4}{32\pi^2 \epsilon_0^2 \hbar^2}, \quad (6)$$

where the right-hand side is the ionization energy in International System of Units units, m is the mass of the lepton, μ is the reduced mass of the atom, q is the electron charge and γ is the Lorentz factor of the produced pairs in the z.m. frame. Therefore the maximum Lorentz factor in the z.m. frame that the particles can have and still form an onium is

$$\gamma_{\text{lim}} = 1 + \frac{q^4}{128\pi^2 c^2 \epsilon_0^2 \hbar^2} = 1 + 6.656 \times 10^{-6}. \quad (7)$$

Thus, only very low energy pairs can produce an onium, and γ_{lim} is independent of mass. We now estimate the fraction of pairs produced with $\gamma < \gamma_{\text{lim}}$, for various formation mechanisms.

III. THE PAIR-PRODUCTION SPECTRUM

Throughout this section we will refer to μ and M , but the arguments are identical for τ and T .

A. Pair production by photon-photon annihilation

For two photons with energy E_1 and E_2 colliding at an angle θ , pair production will occur if

$$E_1 E_2 \geq \frac{2(mc^2)^2}{1 - \cos \theta}, \quad (8)$$

where $m = 2\mu$ is the mass of an individual particle. The total energy of either produced particle, E_0 , is given by

$$E_0^2 = \gamma^2 m^2 c^4 = \frac{E_1 E_2 (1 - \cos \theta)}{2}, \quad (9)$$

where γ is the Lorentz factor of either of the created particles in the z.m. frame.

Many authors [27–31] have evaluated the pair-production spectrum (usually of e^\pm) based on various assumptions about the distributions of photon energies. Here we repeat these calculations, except we integrate the resulting spectra in order to obtain the fraction of produced pairs which have sufficiently low energy to form M , i.e., those which obey Eq. (7).

The total cross section for the reaction $\gamma + \gamma \rightarrow \mu^- + \mu^+$ is [32],

$$\sigma = F_c \frac{q^4}{32\pi\epsilon_0^2 m^2 c^4} (1 - \beta^2) \times \left((3 - \beta^4) \ln \frac{1 + \beta}{1 - \beta} - 2\beta(2 - \beta^2) \right) \quad (10)$$

$$F_c = \frac{\pi \frac{\alpha}{\beta}}{1 - e^{-\pi \frac{\alpha}{\beta}}}, \quad (11)$$

where $\beta = u/c$, and u is the velocity of the outgoing particles in the z.m. frame, and F_c is the Sommerfeld-Sakharov correction to the cross section, due to the attractive Coulomb force between the created μ^\pm , which applies near the threshold energy [33–35]. Now consider a source of photons whose number density per unit energy is given by $n_1(E_1)$. Let these photons interact with an isotropic photon gas whose number density per unit energy is given by $n_2(E_2)$. The fraction of photons in the isotropic gas which lie within a differential cone at angle θ and width $d\theta$ to the incoming photon is $\frac{1}{2} \sin \theta d\theta$. The reaction rate in the lab frame, i.e., the number of pairs created per unit volume per unit time is thus given by

$$R_{\gamma\gamma} = \int_0^\infty \int_{-1}^1 \int_{E_{1\text{min}}}^{E_{1\text{max}}} \times n_1(E_1) n_2(E_2) \sigma(\beta) \frac{c}{2} (1 - \cos \theta) \times dE_1 d \cos \theta dE_2 \quad (12)$$

where the factor $c(1 - \cos \theta)$ is the relative velocity of the incoming photons, and the lower limit on the integral over E_1 ,

$$E_{1\text{min}} = \frac{2m^2 c^4}{E_2 (1 - \cos \theta)} \quad (13)$$

from Eq. (8), ensures pair production is possible. The upper limit on E_1 is either

$$E_{1\text{max}} = E_{1M} = \frac{2\gamma_{\text{lim}}^2 m^2 c^4}{E_2 (1 - \cos \theta)} \quad (14)$$

to specify only the produced pairs which satisfy Eq. (7), or

$$E_{1\text{max}} = E_{1\infty} = \infty \quad (15)$$

for all produced pairs. The fraction of pairs which can produce M , $f_{\gamma\gamma}$, is thus given by the ratio of R integrated over both these limits.

We have evaluated Eq. (12) numerically for different cases of photon energy distribution. Because we are interested in the ratio of R for different limits in γ , and because E_1 and E_2 are related to γ via Eq. (9), the form for the second distribution $n(E_2)$ does not matter; integrating over E_2 leads to a different constant which cancels when taking the ratio. Thus, $f_{\gamma\gamma}$ is identical for a specific power law interacting with any isotropic photon gas. The fraction $f_{\gamma\gamma}$'s for different power-law indices are given in Table II.

B. Pair production by electron-positron annihilation

The total cross section for the process $e^- + e^+ \rightarrow \mu^- + \mu^+$ is given by [36]

TABLE II. The fraction of pairs produced via photon-photon annihilation with sufficiently low energy to form an onium, for photon distributions with a power-law energy density with index $-\alpha$.

α	$f_{\gamma\gamma}^a$
1	2.0×10^{-7}
1.5	3.8×10^{-7}
2	6.1×10^{-7}
2.5	8.9×10^{-7}

^aSince the fraction $f_{\gamma\gamma}$ is independent of mass this is the fraction for any onium, Ps , M or T .

TABLE III. The fraction of pairs produced via electron-positron annihilation with sufficiently low energy to form an onium, for electron distributions with a power-law energy density with index $-\alpha$.

α	f_{ee}^a
1	5.7×10^{-7}
1.5	9.1×10^{-7}
2	1.3×10^{-6}
2.5	1.7×10^{-6}

^aSince the fraction f_{ee} is independent of mass this is the fraction for any onium, Ps, M or T.

$$\sigma = F_c \frac{\pi \alpha^2 \hbar^2 \beta (\beta^4 - 4\beta^2 + 3)}{6M^2 c^2} \quad (16)$$

where M is the muon mass, and F_c is the Sommerfeld-Sakharov factor given by Eq. (11). The fraction of those muons produced which have sufficiently low energy that they could immediately form M now given by

$$R_{ee} = \int_0^\infty \int_{-1}^1 \int_{E_{1\min}}^{E_{1\max}} \times n_1(E_1) n_2(E_2) \sigma(\beta) \frac{v}{2} \times dE_1 d\cos\theta dE_2 \quad (17)$$

where v is the relative speed of the electron and positron in the lab frame and $n_1(E_1)$ and $n_2(E_2)$ are now the distributions of the lab frame number density per unit energy of the electrons and positrons.

The lab frame energies E_1 and E_2 are related to the Lorentz factors of the produced pairs by Eq. (A3), and the relative velocity in the lab frame, v , is given by Eq. (A4). Therefore changing variables to integrate over γ instead of E_1 , we can calculate $R_{ee\gamma_{\lim}}$ in the limit $\gamma_{\max} = \gamma_{\lim}$, and $R_{ee\infty}$ in the limit $\gamma_{\max} = \infty$, and thus the fraction of produced pairs with sufficiently low energy to form M is given by

$$f_{ee} = \frac{R_{ee\gamma_{\lim}}}{R_{ee\infty}}. \quad (18)$$

As for photon-photon annihilation the exact energy density of E_2 does not matter, since it cancels when taking the ratio, and the result is independent of the mass of the produced particles. We have calculated f_{ee} for various power-law indices, where we evaluated the integrals numerically, and we show the results in Table III.

IV. CROSS SECTIONS FOR RADIATIVE RECOMBINATION AND DIRECT ANNIHILATION

In the previous section we calculated the fraction of pairs produced, either via photon-photon annihilation, or by

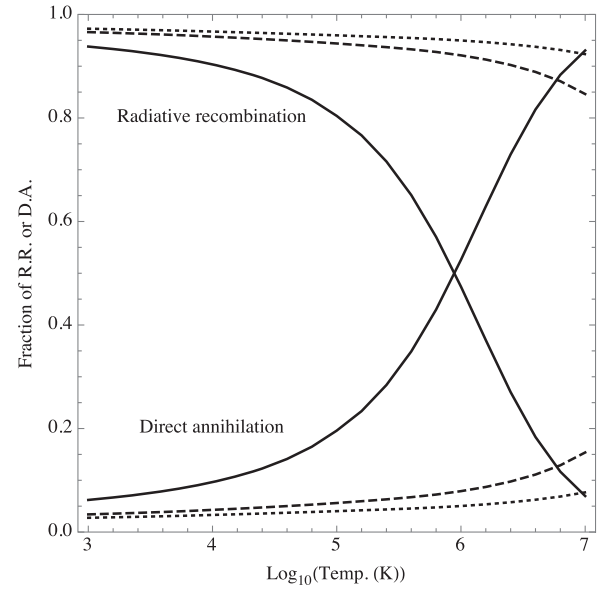


FIG. 1. The fraction of thermalized pairs which will either radiatively recombine (R.R.) or directly annihilate (D.A.), neglecting charge exchange, as a function of temperature, for e^\pm (continuous line), μ^\pm (dashed line) and τ^\pm (dotted line).

electron-positron annihilation, which have sufficiently low energy to form Ps, M or T immediately. However, the fraction of these pairs which will form an onium is less still. As for Ps [21] there is still a probability that some of these pairs will directly annihilate; though in the case of μ and τ we can neglect charge exchange since the probability of the particles decaying before meeting a neutral atom is large.

We have calculated the total reaction rates for radiative recombination and direct annihilation following Gould [21] (see also Gould [37]). Figure 1 shows the fraction of pairs which radiatively recombine, g_{rr} , or directly annihilate, g_{da} , as a function of temperature. For e^\pm radiative recombination dominates below $\approx 10^6$ K, and for μ and τ , radiative recombination dominates at all astrophysically relevant temperatures.

A. Cross sections for radiative recombination onto the nL th level

For those pairs which do radiatively recombine to form an onium, we require the fractions which recombine into the nL th level, such that we may then determine the subsequent decay. Wallyn *et al.* [22] give the cross sections for the formation of Ps via radiative recombination as a function of the quantum levels n and L and the relative energy of the electron and positron. We have repeated these calculations for Ps, M and T, and show the results in Fig. 2. Thus we may calculate the fraction of oniums which form in the nL th energy level via radiative recombination as

V. DECAY CHANNELS

We have now calculated the fraction of pairs produced via photon-photon (Sec. III A), or electron-positron (Sec. III B), annihilation which have sufficiently low energy to form Ps, M or T, and of those which do, the fraction which radiatively recombine or directly annihilate (Sec. IV), and of those which radiatively recombine to form an onium, the fraction which form in the nL th level (Sec. IV A).

An onium in the nL th level may decay via annihilation of its constituent particles, if $L = 0$; it may radiatively transition to a lower quantum level if $n > 1$; or if it is M or T, either one of the individual constituent particles may decay from any level. We wish to calculate the branching fractions for these various decay channels, and we begin by calculating the lifetimes for each process.

A. Annihilation

Invariance under charge conjugation leads to the following selection rule for the decay of an onium into n photons,

$$(-1)^{l+s} = (-1)^n, \quad (20)$$

where l and s are the orbital angular momentum and spin quantum numbers respectively [38,39]. Furthermore, since the electron and positron (or μ^- and μ^+ etc.) only overlap in the $L = 0$ state, annihilation into photons is only possible (barring negligible higher order decay processes) from the singlet 1S_0 state or from the triplet 3S_1 state. The 1S_0 will decay into an even number of photons, with 2 being the most probable. The 3S_1 state will decay into an odd number of photons, with 3 being the most probable, since 1 is forbidden due to conservation of momentum. However, for M and T the triplet state can also decay via one photon, which then decays into e^\pm pairs, i.e., $M \rightarrow \gamma^* \rightarrow e^+e^-$.

The decay rate of an onium in the n th level of the singlet state is given by [40]

$$\Gamma_1 = \frac{1}{n^3} \frac{\alpha^5 \mu c^2}{\hbar}, \quad (21)$$

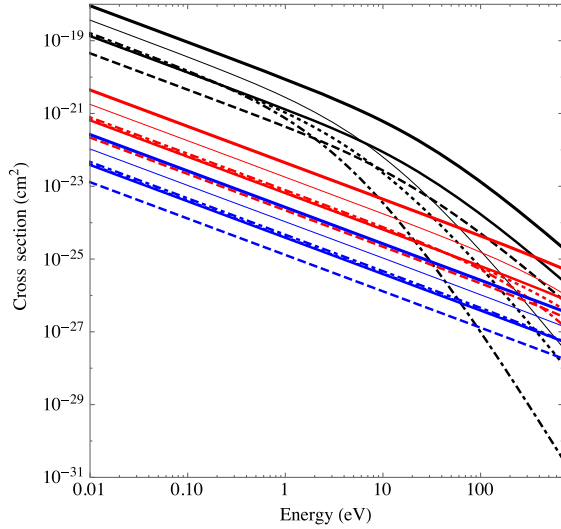
where μ is the reduced mass of the onium.

For triplet states the lowest order decay rate is [41,42]

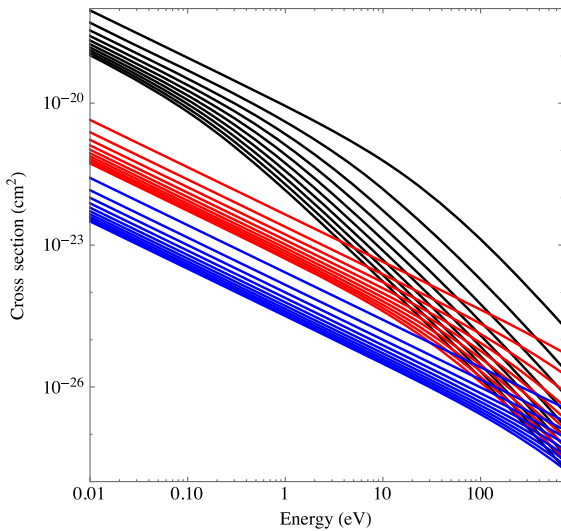
$$\Gamma_3 = \frac{1}{n^3} \frac{2}{9\pi} (\pi^2 - 9) \left(\frac{2\mu c^2}{\hbar} \right) \alpha^6. \quad (22)$$

For M and T the decay of the triplet state into electron-positron pairs has a decay rate given by [20]

$$\Gamma_{e^+e^-} = \frac{\alpha^5 \mu c^2}{3\hbar n^3}. \quad (23)$$



(a) The total cross section for levels nL



(b) The total cross section for level n , summed over all the L sub-levels.

FIG. 2 (color online). (a) The cross section for the radiative recombination of Ps (black), M (red) and T (blue), onto the quantum levels nL for $n = 1$ to 3 as a function of the relative energy of the combining particles. The lines are coded (1,0) thick, (2,0) normal, (2,1) thin, (3,0) dashed, (3,1) dotted, (3,2) dot-dashed. (b) The total cross sections for level n , from $n = 1$ to 10, summed over all the L sublevels.

$$f_{\sigma_{nL}} = \frac{\sigma(nL)}{\sum_{n=1}^{\infty} \sum_{L=0}^{n-1} \sigma(nL)}. \quad (19)$$

In practice we cannot sum to $n = \infty$, and instead choose a suitably high value of $n = n_{\text{lim}}$, such that the fraction $f_{\sigma_{nL}}$ asymptotes to a constant value. We computed $f_{\sigma_{nL}}$ for various limits, n_{lim} , and found that $n_{\text{lim}} = 300, 500$ or 1000 is sufficient for Ps, M or T respectively. Using these limits we have calculated the fractions $f_{\sigma_{nL}}$ for Ps, M and T as a function of temperature, and give the results for the first six energy levels in Table IV.

TABLE IV. The fraction of those atoms which radiatively recombine to form Ps, M or T, which do so in the level nL .

		Temperature (K)														
		Ps					M					T				
n	L	10 ³	10 ⁴	10 ⁵	10 ⁶	10 ⁷	10 ³	10 ⁴	10 ⁵	10 ⁶	10 ⁷	10 ³	10 ⁴	10 ⁵	10 ⁶	10 ⁷
1	0	0.296	0.459	0.702	0.814	0.830	0.153	0.193	0.263	0.396	0.628	0.123	0.145	0.182	0.244	0.358
2	0	0.043	0.068	0.100	0.105	0.104	0.022	0.028	0.039	0.059	0.093	0.018	0.021	0.027	0.036	0.053
2	1	0.116	0.143	0.068	0.009	0.001	0.062	0.078	0.105	0.140	0.102	0.050	0.058	0.073	0.097	0.133
3	0	0.015	0.023	0.031	0.031	0.031	0.008	0.010	0.013	0.020	0.029	0.006	0.007	0.009	0.012	0.018
3	1	0.044	0.055	0.025	0.003	0.000	0.023	0.030	0.040	0.053	0.038	0.019	0.022	0.028	0.037	0.051
3	2	0.048	0.037	0.003	0.000	0.000	0.027	0.034	0.045	0.046	0.010	0.022	0.026	0.032	0.042	0.049
4	0	0.007	0.010	0.013	0.013	0.013	0.004	0.004	0.006	0.009	0.013	0.003	0.003	0.004	0.006	0.008
4	1	0.021	0.026	0.011	0.001	0.000	0.011	0.014	0.019	0.025	0.017	0.009	0.011	0.013	0.018	0.024
4	2	0.030	0.023	0.002	0.000	0.000	0.017	0.021	0.028	0.029	0.006	0.014	0.016	0.020	0.026	0.030
4	3	0.020	0.007	0.000	0.000	0.000	0.013	0.016	0.020	0.013	0.001	0.010	0.012	0.015	0.019	0.017
5	0	0.004	0.006	0.007	0.007	0.007	0.002	0.003	0.003	0.005	0.007	0.002	0.002	0.002	0.003	0.005
5	1	0.012	0.014	0.006	0.001	0.000	0.006	0.008	0.011	0.014	0.009	0.005	0.006	0.007	0.010	0.013
5	2	0.018	0.014	0.001	0.000	0.000	0.010	0.013	0.017	0.017	0.004	0.008	0.010	0.012	0.016	0.019
5	3	0.017	0.007	0.000	0.000	0.000	0.011	0.014	0.017	0.012	0.001	0.009	0.011	0.013	0.017	0.015
5	4	0.008	0.001	0.000	0.000	0.000	0.006	0.008	0.009	0.003	0.000	0.005	0.006	0.007	0.009	0.005
6	0	0.002	0.003	0.004	0.004	0.004	0.001	0.002	0.002	0.003	0.004	0.001	0.001	0.001	0.002	0.003
6	1	0.007	0.008	0.003	0.000	0.000	0.004	0.005	0.007	0.008	0.005	0.003	0.004	0.005	0.006	0.008
6	2	0.012	0.009	0.001	0.000	0.000	0.007	0.008	0.011	0.011	0.002	0.005	0.006	0.008	0.010	0.012
6	3	0.013	0.005	0.000	0.000	0.000	0.008	0.010	0.013	0.009	0.000	0.007	0.008	0.010	0.012	0.011
6	4	0.009	0.001	0.000	0.000	0.000	0.007	0.009	0.010	0.004	0.000	0.006	0.007	0.008	0.010	0.006
6	5	0.003	0.000	0.000	0.000	0.000	0.003	0.004	0.004	0.001	0.000	0.002	0.003	0.004	0.004	0.001

B. Decay

Both the μ and the τ lepton are intrinsically unstable and will decay to lighter particles. We take the decay rates to be $T_\mu = 1/\Gamma_\mu = 2.197 \times 10^{-6}$ s and $T_\tau = 1/\Gamma_\tau = 2.874 \times 10^{-13}$ s [36].

$$\nu = cR_\infty \left(\frac{1}{n^2} - \frac{1}{n'^2} \right), \tag{25}$$

R_∞ is the Rydberg constant for the particular onium,

C. Radiation

The coefficient for a radiative transition of a hydrogenic atom from the state $n'L'$ to a lower state nL , $A_{n'L',nL}$ is given by [43–45]

$$R_\infty = \frac{(\mu e^4)}{8\epsilon_0^2 c \hbar^3}, \tag{26}$$

and a_0 is the Bohr radius of the onium,

$$A_{n'L',nL} = 4\pi^2 \nu^3 \left(\frac{8\pi\alpha a_0^2}{3c^2} \right) \frac{\text{Max}(L, L')}{(2L' + 1)} |p(n'L', nL)|^2, \tag{24}$$

$$a_0 = \frac{4\pi\epsilon_0 \hbar^2}{\mu e^2}. \tag{27}$$

where ν is the frequency of the transition,

The dipole matrix elements are given by [46]

$$|p(n'L - 1, nL)|^2 = \left(\frac{(-1)^{n'-1}}{4(2L - 1)!} \sqrt{\frac{(n + L)!(n' + L - 1)!}{(n - L - 1)!(n' - L)!}} \frac{(4nn')^{L+1}}{(n + n')^{n+n'}} (n - n')^{n+n'-2L-2} \right. \\ \times \left({}_2F_1 \left[-n + L + 1, -n' + L, 2L, \frac{-4nn'}{(n - n')^2} \right] \right. \\ \left. \left. - \left(\frac{n - n'}{n + n'} \right)^2 {}_2F_1 \left[-n + L - 1, -n' + L, 2L, \frac{-4nn'}{(n - n')^2} \right] \right) \right)^2, \tag{28}$$

which is correct when $L > L'$; if $L < L'$ then nL and $n'L'$ are swapped. These can be adapted for any onium simply by replacing the reduced mass, μ [22].

The radiative coefficient for a transition from a level $n'L'$ to *any* lower level is thus given by

$$A_{n'L'} = \sum_{n=1}^{n=n'-1} \sum_{L=L'\pm 1} A_{n'L',nL}. \quad (29)$$

VI. BRANCHING RATIOS

A. Branching ratios for a particular level, nL

Consider leptonium in the level nL . It may decay via annihilation (two photon, three photon or e^\pm , depending on the state and the type of atom), radiative transition, or the decay of either constituent particle (for M and T). The decay rates for these channels were calculated in the previous section. Thus we may now calculate the probabilities for each process.

Recalling that annihilation can only take place from the states with $L = 0$, and also that the annihilation mechanisms differ for singlet states, which decay into two photons, and triplet states, which decay either into three photons or into e^\pm pairs via a single photon, the total decay constant for leptonium in a level nL via *any* decay process is given by

$$A_{nL_{\text{sing}}} = A_{nL} + \delta(L)\Gamma_1 + 2\Gamma_{\mu,\tau}, \quad {}^1S_0, \quad (30)$$

$$A_{nL_{\text{trip}}} = A_{nL} + \delta(L)\Gamma_3 + \delta(L)\Gamma_{ee} + 2\Gamma_{\mu,\tau}, \quad {}^3S_1, \quad (31)$$

where $\delta(L)$ is a function which is 1 when $L = 0$, and zero otherwise.

Therefore the probability of making a particular radiative transition from a level $n'L'$ to a lower level nL is given by

$$P_{n'L',nL_{\text{sing}}} = \frac{1}{4} \frac{A_{n'L',nL}}{A_{n'L'_{\text{sing}}}}, \quad (32)$$

$$P_{n'L',nL_{\text{trip}}} = \frac{3}{4} \frac{A_{n'L',nL}}{A_{n'L'_{\text{trip}}}}, \quad (33)$$

$$P_{n'L',nL_{\text{tot}}} = P_{n'L',nL_{\text{sing}}} + P_{n'L',nL_{\text{trip}}}, \quad (34)$$

where the leading factors of 1/4 and 3/4 are the probabilities that the onium will form in the singlet or triplet state respectively.

Similarly the probability for leptonium in the level $n'L'$ to decay via two photon annihilation is

$$P_{n'L'_{\text{sing}}} = \frac{1}{4} \frac{\delta(L')\Gamma_1}{A_{n'L'_{\text{sing}}}}. \quad (35)$$

Likewise for three photon annihilation,

$$P_{n'L'_{\text{trip}}} = \frac{3}{4} \frac{\delta(L')\Gamma_3}{A_{n'L'_{\text{trip}}}}, \quad (36)$$

and annihilation into an electron-positron pair

$$P_{n'L'_{\text{ee}}} = \frac{3}{4} \frac{\delta(L')\Gamma_{ee}}{A_{n'L'_{\text{trip}}}}. \quad (37)$$

Finally the probability that either constituent particle will decay is

$$P_{n'L'_{\text{decay}}} = 2 \left(\frac{\Gamma_{\mu,\tau}}{4} \frac{1}{A_{n'L'_{\text{sing}}}} + \frac{3}{4} \frac{\Gamma_{\mu,\tau}}{A_{n'L'_{\text{trip}}}} \right) \quad (38)$$

where $\Gamma_{\mu,\tau}$ is the decay rate of the μ or τ as appropriate.

B. Total branching ratios

The previous subsection gave the branching ratios for the various decays from a particular state nL . We now need to consider the probability of leptonium being in the state nL in the first place. There are two possibilities for populating the state: it may recombine directly into the state nL , or it may recombine into a higher state and cascade down into nL . That is, we assume case A recombination [47]; because leptonium is short lived, there is no resonant scattering of emission lines from Ps, M or T, through the excitation and reemission of surrounding Ps, M or T atoms. For the same reason, we also assume that collisional excitation of the atoms is negligible.

1. Cascade probabilities

The probability of cascading from a level $n'L'$ to a lower level nL via *all* cascade paths, $C_{n'L',nL}$, is calculated using an iterative procedure [44], such that

$$C_{n'L',nL_{\text{sing,trip}}} = \begin{cases} 1, & n = n' \wedge L = L', \\ \sum_{n''=n}^{n'-1} \sum_{L''=L'\pm 1} P_{n'L',n''L''_{\text{sing,trip}}} C_{n''L'',nL_{\text{sing,trip}}}, & n \neq n' \vee L \neq L', \end{cases} \quad (39)$$

where the subscripts “sing” and “trip” are used to specify the calculations for the singlet state or triplet state, an unfortunate but necessary complication since the decay paths are different for each.

2. Population of the state, nL

Meanwhile the state is depopulated by the processes described in Sec. V. Therefore, in equilibrium the population of any state, N_{nL} is given by [44,48]

$$\begin{aligned} & \sum_{n'=n}^{\infty} \sum_{L'=0}^{n'-1} N_{\text{pairs}} f_{\text{ion}} g_{\text{rr}} f_{\sigma_{nL}} C_{n'L',nL_{\text{sing,trip}}} \\ &= N_{nL_{\text{sing,trip}}} A_{nL_{\text{sing,trip}}}, \end{aligned} \quad (40)$$

where N_{pairs} is the rate at which pairs are produced, f_{ion} is the fraction of pairs produced with energy less than the ionization energy, i.e., $f_{\gamma\gamma}$ or f_{ee} in Secs. III A and III B above, g_{rr} is the fraction of those pairs which radiatively recombine (Sec. IV, Fig. 1), $f_{\sigma_{nL}}$ is the fraction of those pairs which form in level nL , [Sec. IV A, Eq. (19)], and again the equation has two forms reflecting the different decay paths of the singlet and triplet states.

Let us then define f_{nL} as the relative population of the level nL , i.e.,

$$\begin{aligned} f_{nL_{\text{sing,trip}}} &= \frac{N_{nL_{\text{sing,trip}}}}{N_{\text{pairs}} f_{\text{ion}} g_{\text{rr}}} \\ &= \frac{\sum_{n'=n}^{\infty} \sum_{L'=0}^{n'-1} f_{\sigma_{n'L'}} C_{n'L',nL_{\text{sing,trip}}}}{A_{nL_{\text{sing,trip}}}}, \end{aligned} \quad (41)$$

which is the fraction of leptonium in the level nL for a population whose formation and decay rates are in equilibrium.

3. Branching ratios

The final step in calculating the total branching ratios is simply to multiply the fractional population each state, f_{nL} , by the appropriate decay constant, and sum over all levels. Thus,

$$P_{\text{Ly}\alpha} = A_{21,10} \left(\frac{1}{4} f_{21_{\text{sing}}} + \frac{3}{4} f_{21_{\text{trip}}} \right), \quad \text{Lyman}\alpha, \quad (42)$$

$$P_{\text{Ly}\beta} = A_{31,10} \left(\frac{1}{4} f_{31_{\text{sing}}} + \frac{3}{4} f_{31_{\text{trip}}} \right), \quad \text{Lyman}\beta, \quad (43)$$

$$P_{\text{Ba}\alpha} = A_{31,20} \left(\frac{1}{4} f_{31_{\text{sing}}} + \frac{3}{4} f_{31_{\text{trip}}} \right) + A_{30,21} \left(\frac{1}{4} f_{30_{\text{sing}}} + \frac{3}{4} f_{30_{\text{trip}}} \right), \quad \text{Balmer}\alpha, \quad (44)$$

$$P_{\text{Ba}\beta} = A_{41,20} \left(\frac{1}{4} f_{41_{\text{sing}}} + \frac{3}{4} f_{41_{\text{trip}}} \right) + A_{40,21} \left(\frac{1}{4} f_{40_{\text{sing}}} + \frac{3}{4} f_{40_{\text{trip}}} \right), \quad \text{Balmer}\beta, \quad (45)$$

$$P_{\gamma\gamma} = \sum_{n=0}^{\infty} \frac{1}{4} f_{n0_{\text{sing}}} \Gamma_1(n), \quad \text{two photon annihilation}, \quad (46)$$

$$P_{\gamma\gamma\gamma} = \sum_{n=0}^{\infty} \frac{3}{4} f_{n0_{\text{trip}}} \Gamma_3(n), \quad \text{three photon annihilation}, \quad (47)$$

$$P_{ee} = \sum_{n=0}^{\infty} \frac{3}{4} f_{n0_{\text{trip}}} \Gamma_{ee}(n), \quad \text{electron-positron annihilation}, \quad (48)$$

$$P_{\text{decay}} = \sum_{n=0}^{\infty} \sum_{L=0}^{n-1} 2\Gamma_{\mu,\tau} \left(\frac{1}{4} f_{nL_{\text{sing}}} + \frac{3}{4} f_{nL_{\text{trip}}} \right), \quad \text{decay of either particle}. \quad (49)$$

All of Eqs. (42)–(49), contain either one or two infinite sums. All include the infinite sum in Eq. (41) which accounts for recombination into any level up $n = \infty$ followed by cascade to the relevant level. Equations (46)–(49) also include the sum over all levels up to $n = \infty$ which all contribute to the relevant decay process. In

practice we cannot compute these infinite sums, and instead compute Eqs. (42)–(49) up to certain limits on each sum. We then alter these limits, and fit to the resulting curve or surface, and extrapolate our results to $n = \infty$. The limits are $n = 11$ – 15 , for the capture-cascade sum, and $n = 6$ – 10 for the sum over the decays.

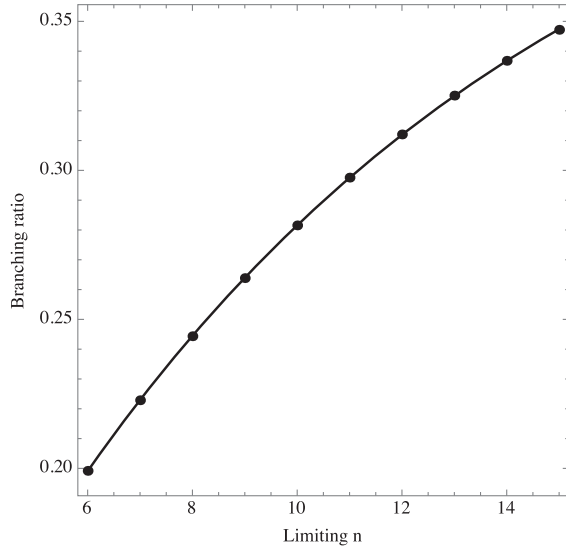


FIG. 3. The branching ratio of Ly α emission from M at a gas temperature of $T = 10^4$ K as a function of the limiting value of the sum over n in Eq. (41), shown by the points. We find good fits with a function of the form given in Eq. (50), shown by the curve, in this case giving a limiting value as $n \rightarrow \infty$ of 0.45.

For example, Fig. 3 shows the fit to the branching ratio for M emitting Lyman α radiation at a gas temperature of $T = 10^4$ K. We find a good fit to all curves using a function of the form

$$b = a + ce^{-\frac{n}{d}}, \quad (50)$$

where a , c and d are all parameters to be fit. Figure 4 shows the two-dimensional fit over both limits for annihilation into electron-positron pairs for M at $T = 10^4$ K. Again, we find a good fit with a functional form

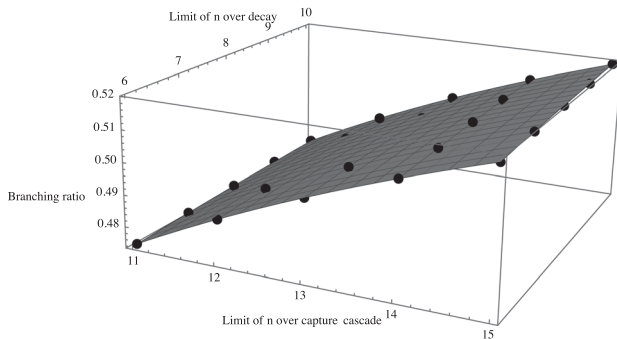


FIG. 4. The branching ratio of decay into an electron-positron pair from M at a gas temperature of $T = 10^4$ K as a function of the limiting value of the sums over n in Eqs. (41) and (48), shown by the points. We find good fits with a function of the form given in Eq. (51), shown by the curve, in this case giving a limiting value as $n \rightarrow \infty$ of 0.59.

$$b = a + ce^{-\frac{n_1}{d}} + fe^{-\frac{n_2}{g}}, \quad (51)$$

where a , c , d , f and g are all parameters to be fit, and the n_1 and n_2 are the different limiting values of n in the sums.

We have checked the accuracy of the extrapolations in the following way. The branching ratios for the two photon or three photon decay of Ps should be 0.25 and 0.75 by definition, since there is no other way for Ps to decay. We find the values given in Table V, which agree to within 2 percent in all cases.

We wish to highlight one further caveat to these branching ratios. The extrapolations for photon decays and electron-positron decays are not large, and become less important as n increases, since they can only occur when $L = 0$, which becomes less common for a higher n . However, the decay of either particle can occur from any L level, and the extrapolations are large and therefore uncertain. Therefore, rather than rely on the extrapolations for decay, we set the probability to be one minus the sum of the other decays. In any case, the decay of either particle does not have a clear observational signature and it is the probabilities for the other processes which are most important for this study. This uncertainty in our results could be lessened through calculations to higher levels, but would require significant computing resources, which are unavailable to us at this time.

The results for the branching ratios are given in Tables V, VI and VII. Since Ps is well studied and understood, we do not discuss it further [14,22].

M has significant probabilities of Lyman α and Balmer α radiation before decaying. The decay processes are dominated by two photon annihilation for para-M and electron-positron annihilation for ortho-M, as well as significant probabilities for either μ^\pm to decay if $T < 10^5$ K.

The much shorter lifetimes of τ means that the decay processes of T are dominated by the decay of either τ^\pm , with only a small probability of either electron-positron or two photon annihilation. The probabilities of emitting Lyman α radiation before decay are 1 to 2 per cent, and ≈ 0 for other emission lines.

TABLE V. Total branching ratios for Ps as a function of temperature.

T (K)	Ly α	Ly β	Balmer α	Balmer β	Two photon decay	Three photon decay
1000	0.46	0.08	0.24	0.06	0.24	0.73
10000	0.29	0.07	0.09	0.03	0.25	0.74
100000	0.11	0.03	0.03	0.01	0.25	0.75
1000000	0.04	0.01	0.02	0.01	0.25	0.75
10000000	0.03	0.01	0.02	0.01	0.25	0.75

TABLE VI. Total branching ratios for M as a function of temperature.

T (K)	Ly α	Ly β	Balmer α	Balmer β	Two photon decay	Three photon decay	Electron-positron decay	Decay of either particle
1000	0.37	0.04	0.27	0.04	0.16	0.00	0.48	0.36
10000	0.45	0.05	0.31	0.05	0.20	0.00	0.59	0.21
100000	0.46	0.07	0.26	0.06	0.23	0.00	0.70	0.07
1000000	0.32	0.07	0.12	0.04	0.25	0.00	0.74	0.01
10000000	0.13	0.04	0.02	0.01	0.25	0.00	0.74	0.00

TABLE VII. Total branching ratios for T as a function of temperature.

T (K)	Ly α	Ly β	Balmer α	Balmer β	Two photon decay	Three photon decay	Electron-positron decay	Decay of either particle
1000	0.01	0.00	0.00	0.00	0.03	0.00	0.06	0.91
10000	0.01	0.00	0.00	0.00	0.03	0.00	0.07	0.90
100000	0.01	0.00	0.00	0.00	0.04	0.00	0.09	0.87
1000000	0.01	0.00	0.00	0.00	0.06	0.00	0.12	0.83
10000000	0.02	0.00	0.00	0.00	0.08	0.00	0.17	0.75

VII. OBSERVABLE SIGNATURES

Tables VI and VII give the branching ratios for the possible radiative recombination lines and decays of M and T. We now discuss the observational signatures of these processes. The energies of radiative recombination lines and of two photon annihilation signatures and ionization are given in Table I. In addition to the two photon annihilation signature there will be a continuum of radiation from the three photon decay of the singlet state, with energies from zero to the energy of the two photon decay. The decay mechanisms for both τ and μ are numerous and there is no one clear observable signature that we can associate with either of these, nor is there any single identifiable signature of annihilation into e^\pm .

All these signatures are observable with current instrumentation if they are sufficiently bright. For example Fermi-LAT is sensitive to γ -rays between 30 MeV to 300 GeV and could observe the annihilation of M and T; INTEGRAL IBIS is sensitive to the T Lyman lines; XMM-Newton is sensitive to x-rays between 0.1 and 15 keV, and can observe the recombination lines of M, and the T Balmer lines.

VIII. EXPECTED SIGNATURES FROM ASTROPHYSICAL SOURCES

We are finally in a position to estimate the expected observable signatures of M and T from astrophysical sources. Consider a source of particle-antiparticle pairs being produced at a rate r per second. The fraction of these pairs which will produce M or T is given by

$$f_{\text{onium}} = r f_{\text{ion}} g_{\text{rr}} \quad (52)$$

where f_{ion} is the fraction of pairs produced with energy less than the ionization energy, i.e., $f_{\gamma\gamma}$ or f_{ee} in Secs. III A and III B above, and g_{rr} is the fraction of those pairs which radiatively recombine (Sec. IV, Fig. 1). Therefore the luminosity of any particular observable signature in ph s^{-1} is

$$L = p f_{\text{onium}} b \quad (53)$$

where b is the branching ratio of the particular signature (Tables VI and VII), and p is a factor which specifies the number of photons produced by the process, i.e., $p = 1$ for recombination lines, $p = 2$ for two photon annihilation and $p = 3$ for three photon annihilation. These luminosities can be easily converted to units of erg s^{-1} using the energies of the emitted photons given in Table I.

We will now estimate the expected fluxes from particular sources. These should be compared to the limiting sensitivities of current instruments. The M recombination lines are all in the soft x-ray band (0.5–2 keV), for which a 100 ksec observation has a $\approx 4\sigma$ limiting sensitivity [49] of $f_{\text{X}} \sim 3.1 \times 10^{-16} \text{ erg cm}^{-2} \text{ s}^{-1}$. The T recombination Balmer lines are in the hard x-ray band (2–10 keV), for which a 100 ksec observation has a $\approx 4\sigma$ limiting sensitivity of $f_{\text{X}} \sim 1.4 \times 10^{-15} \text{ erg cm}^{-2} \text{ s}^{-1}$. The T Lyman lines are at the low energy limit of the SPI spectrometer on board INTEGRAL. The limiting 4σ sensitivity for an exposure time of 10^5 s is $\approx 3 \times 10^{-13} \text{ erg cm}^{-2} \text{ s}^{-1}$, using data from the INTEGRAL Web site. The M and T annihilation lines are detectable by FERMI-LAT, for which the limiting 4σ sensitivity for an exposure time of 10^5 s is $\approx 4 \times 10^{-13} \text{ erg cm}^{-2} \text{ s}^{-1}$ for M and $\approx 1 \times 10^{-13} \text{ erg cm}^{-2} \text{ s}^{-1}$ for T, using data from the FERMI Web site.

A. Jets

The powerful relativistic jets of AGN and microquasars are a probable source of pair production. These jets have strong radio emission with a power-law spectrum which is interpreted as being due to synchrotron emission from relativistic e^- gyrating around the magnetic field lines of the AGN. The jets must be electrically neutral, otherwise they would cause a potential difference to be built up, which would oppose and eventually stop the jet.

It is unknown whether the positive component of jets consists of positrons, protons or a mixture of both. Observational studies have had to rely on indirect methods of searching for the presence of e^+ , such as estimates of the bulk kinetic energy contained in jets, which have been used to argue for both e^- -p plasma [50] and e^- - e^+ plasma [51–53].

Theoretically there are good reasons to expect that jets contain some fraction of e^+ . A pair plasma has the advantage of explaining γ -ray jets [54] and the very high Lorentz factors ($\Gamma > 5$) required to account for superluminal bulk velocities of jets [55].

It is possible that some Ps may form in the jet, or similarly, that some e^+ pairs may collide with the required energy to form M and T as outlined in Sec. III B. However, in the observers frame, the velocity of the oniums thus formed will be highly relativistic, causing relativistic Doppler broadening and beaming of any emitted radiation [56,57]. Such a broadened signal may still be possible to observe [56], but would be difficult to interpret, and hardly constitutes an unambiguous test of the presence of exotic onium atoms such as M or T. Therefore we do not consider onium formation in the jet itself as a likely candidate for detection.

However, if a jet collides with a stationary object such as a gas cloud or a star, then the leptonium formed in the collision will give rise to an emission that is in principle observable. Such collisions may occur in the radio jets of AGN [58], or if the jets of microquasars are misaligned and hit the secondary companion [59].

Let us consider some illustrative examples. Previously [12], we have calculated the expected positron contents of jets, by applying the arguments of Marscher *et al.* [57] and

TABLE VIII. The intrinsic luminosities for a blazar jet which produces $10^{49} e^+ s^{-1}$, with spectral index $\alpha = 1.5$ and $T = 10^6$ K.

	Luminosity (ph s^{-1})	
	M	T
Ly α	2.7×10^{42}	1.2×10^{41}
Ly β	6.0×10^{41}	1.3×10^{40}
Ba α	9.8×10^{41}	7.7×10^{39}
Ba β	3.3×10^{41}	1.6×10^{39}
Two photon	4.1×10^{42}	9.6×10^{41}

Marscher [60], which were developed in order to search for 511 keV Ps annihilation radiation from 3C 120, to the empirical measurements of Ghisellini [61]. We found a maximum of $\approx 10^{49} e^+ s^{-1}$ are produced in the jets of blazars, whereas quasars produce $\approx 10^{46}$ – $10^{48} e^+ s^{-1}$ in their jets. The jets of microquasars are expected to have a positron flux of $\approx 10^{41} e^+ s^{-1}$ [59]. We assume that the object being hit by the jet is dense enough to stop *all* these positrons. Let us assume a spectral index of $\alpha = 1.5$ and a temperature of $T = 10^6$ K for the positrons in the jet. Thus the intrinsic luminosities of the various observational signatures can be calculated, and are given in Table VIII

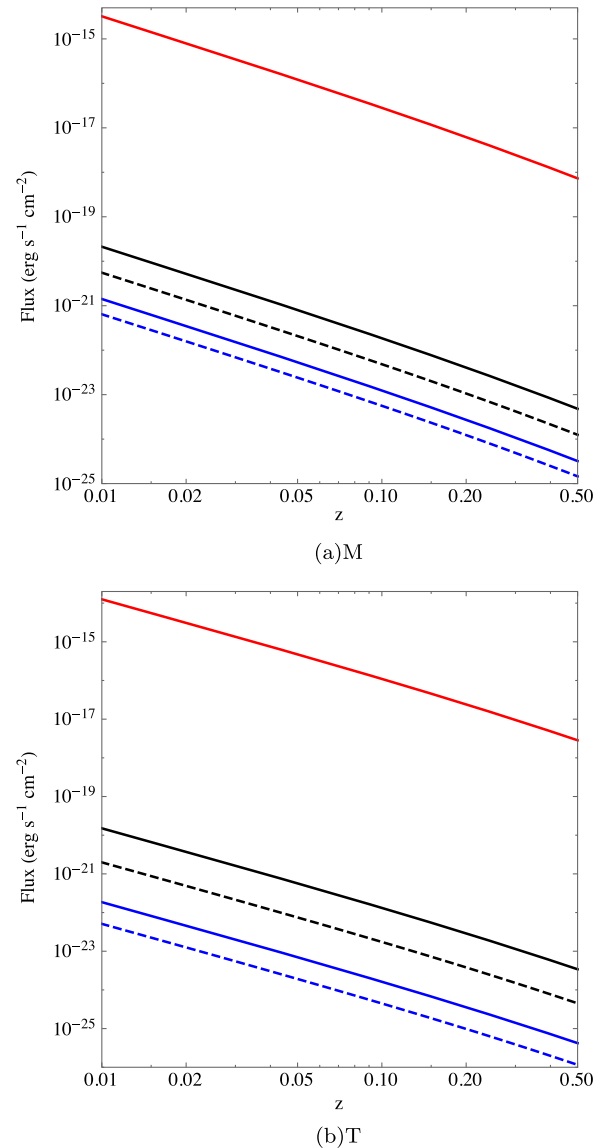


FIG. 5 (color online). The flux as a function of redshift for a blazar jet which produces $10^{49} e^+ s^{-1}$, with spectral index $\alpha = 1.5$ and $T = 10^6$ K, colliding with a gas cloud. The lines show two photon annihilation (red), Ly α (black), Ly β (dashed, black), Ba α (blue) and Ba β (dashed, blue).

TABLE IX. The intrinsic luminosities for a microquasar jet which produces $10^{41} e^+ s^{-1}$, with spectral index $\alpha = 1.5$ and $T = 10^5$ K.

	Luminosity (ph s^{-1})	
	M	T
Ly α	3.9×10^{34}	8.7×10^{32}
Ly β	5.8×10^{33}	9.7×10^{31}
Ba α	2.3×10^{34}	5.9×10^{31}
Ba β	4.8×10^{33}	1.2×10^{32}
Two photon	4.0×10^{34}	7.2×10^{33}

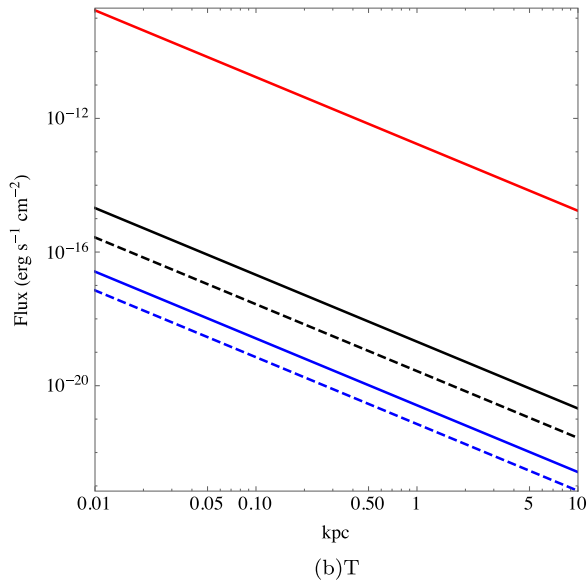
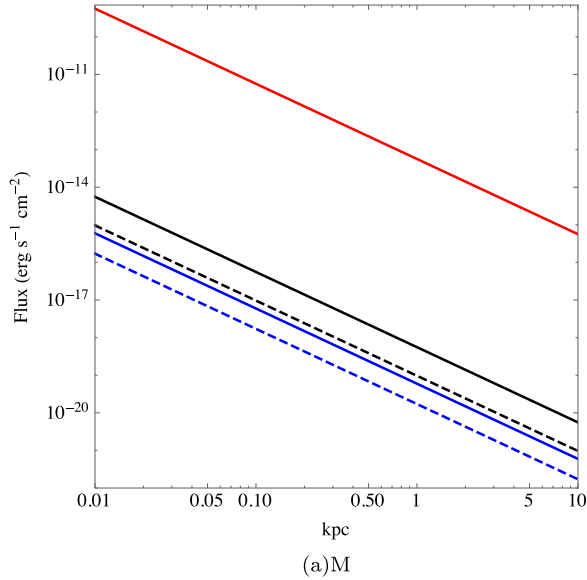


FIG. 6 (color online). The flux as a function of redshift for a microquasar jet which produces $10^{41} e^+ s^{-1}$, with spectral index $\alpha = -1.5$ and $T = 10^5$ K, colliding with a gas cloud. The lines show two photon annihilation (red), Ly α (black), Ly β (dashed, black), Ba α (blue) and Ba β (dashed, blue).

for a blazar. These are then used to calculate the flux of the signal as a function of redshift, as shown in Fig. 5. Similar results are shown in Table IX and Fig. 6, for a misaligned microquasar with a spectral index of $\alpha = 1.5$ and a temperature of $T = 10^5$ K for the positrons in the jet.

For our illustrative examples, no lines from blazars are above the relevant current 4σ detection limits for a 100 ks exposure for either M or T. However, a microquasar jet which produces $10^{41} e^+ s^{-1}$, with spectral index $\alpha = -1.5$ and $T = 10^5$ K, colliding with a gas cloud, would be detectable in principle to the distances given in Table X. The recombination lines would only be detectable at very close distances, but the two photon annihilation should be detectable at 4σ in a 100 ksec exposure to ≈ 0.4 kpc and ≈ 1 kpc for M and T respectively.

TABLE X. The distance to which a microquasar jet which produces $10^{41} e^+ s^{-1}$, with spectral index $\alpha = -1.5$ and $T = 10^5$ K, colliding with a gas cloud, would be detectable at 4σ in 100 ksec.

	Distance (kpc)	
	M	T
Ly α	0.04	9×10^{-4}
Ly β	0.01	3×10^{-4}
Ba α	0.01	0.001
Ba β	0.007	7×10^{-4}
Two photon	0.40	1.13

TABLE XI. The number of pairs produced through photon-photon annihilation in an accretion disk.

	AGN	Microquasar
μ	1.7×10^{52}	1.7×10^{42}
τ	5.0×10^{54}	5.0×10^{44}

TABLE XII. The intrinsic luminosities for pair production via photon annihilation in accretion disks surrounding a microquasar and an AGN, assuming solar masses of 10 and $10^6 M_{\odot}$ respectively, temperatures of 10^5 and 10^6 K, and a spectral index of $\alpha = 1.5$.

	Microquasar Luminosity (ph s^{-1})		AGN Luminosity (ph s^{-1})	
	M	T	M	T
Ly α	2.9×10^{35}	1.8×10^{36}	2.0×10^{45}	2.4×10^{46}
Ly β	4.2×10^{34}	2.0×10^{35}	4.4×10^{44}	2.7×10^{45}
Ba α	1.7×10^{35}	1.2×10^{35}	7.2×10^{44}	1.6×10^{45}
Ba β	3.6×10^{34}	2.5×10^{34}	2.4×10^{44}	3.2×10^{44}
Two photon	2.9×10^{35}	1.5×10^{37}	3.0×10^{45}	2.0×10^{47}

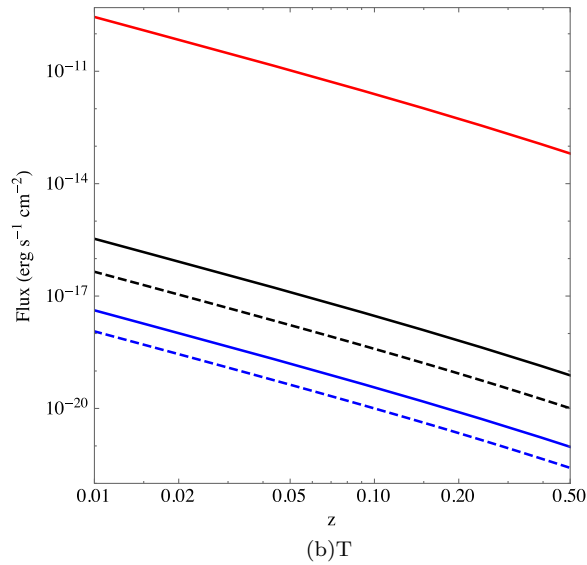
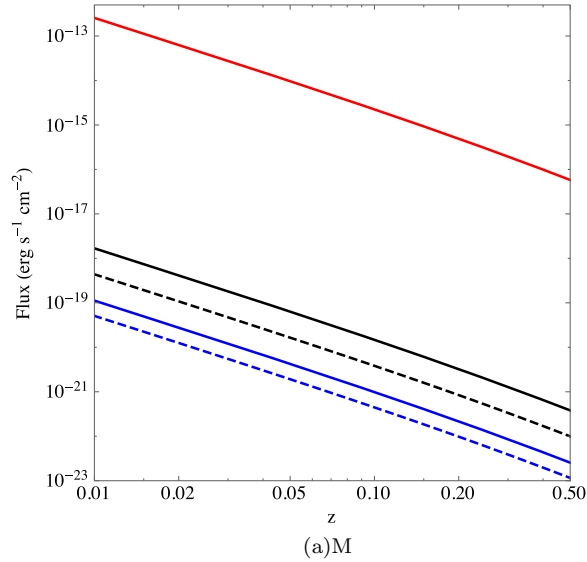


FIG. 7 (color online). The flux as a function of redshift for an accretion disk around an AGN with a $10^6 M_\odot$ black hole, and spectral index $\alpha = 1.5$ and $T = 10^6$ K. The lines show two photon annihilation (red), Ly α (black), Ly β (dashed, black), Ba α (blue) and Ba β (dashed, blue).

B. Accretion disks

We now consider pairs produced in the accretion disk itself through photon-photon annihilation. The number density of pairs thus produced in the optically thick region of the disk is

$$N_{\gamma\gamma} \sim \frac{1}{\sigma_T R}, \quad (54)$$

where σ_T is the Thompson cross section for μ or τ and R is the radius of the optically thick disk [62]. If we assume $R \approx 2GM/c^2$, i.e., the disk has approximately the

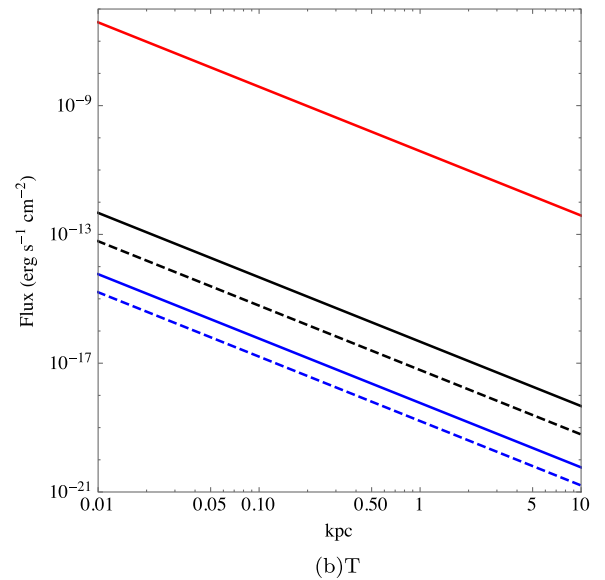
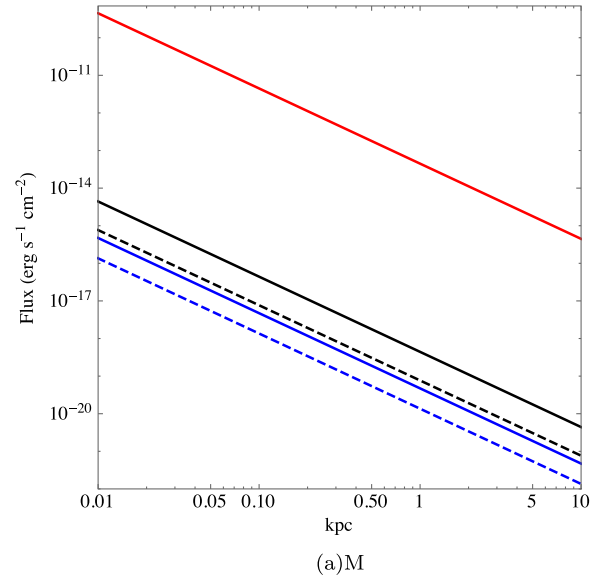


FIG. 8 (color online). The flux as a function of redshift for an accretion disk around a microquasar with a $10 M_\odot$ black hole, and spectral index $\alpha = 1.5$ and $T = 10^5$ K. The lines show two photon annihilation (red), Ly α (black), Ly β (dashed, black), Ba α (blue) and Ba β (dashed, blue).

Schwarzschild radius and the thickness of the disk is $\approx R$, then taking masses of $M_{\text{AGN}} = 10^6 M_\odot$ for the mass of a black hole in an AGN, and $M_{\mu\text{QSO}} = 10 M_\odot$ for the mass of a black hole in a microquasar, then the pair yields are as given in Table XI.

Now, assuming a spectral index of $\alpha = 1.5$, then we may estimate the branching ratios as in Eq. (53), whereupon we find the luminosities in ph s^{-1} , as listed in Table XII. The flux of the AGN as a function of redshift, and the flux of the microquasar as a function of distance, are shown in Figs. 7 and 8.

TABLE XIII. The distance to which an accretion disk around a microquasar with a $10M_{\odot}$ black hole, and spectral index $\alpha = 1.5$ and $T = 10^5$ K, would be detectable at 4σ in 100 ksec.

	Distance (kpc)	
	M	T
Ly α	0.11	0.04
Ly β	0.05	0.01
Ba α	0.04	0.06
Ba β	0.02	0.03
Two photon	1.1	51

For these illustrative examples, and a 4σ detection limit for a 100 ks exposure, the two photon annihilation line of M would be observable in the accretion disk of an AGN at $z < 0.025$, while the two photon annihilation line of T would be observable out to $z < 0.9$. Neither the M nor the T recombination lines would be detectable.

Meanwhile, for microquasars the M and T lines would be detectable at 4σ in a 100 ksec exposure to the distances given in Table XIII. The recombination lines are detectable at close distances while the two photon annihilation should be detectable to 1.1 and 51 kpc for M and T respectively.

IX. CONCLUSIONS

True muonium and true tauonium are the most compact pure QED systems, but have never been observed. Unlike Ps, for which there are extensive observations in our own Galaxy [14], both the formation and decay of M and T are affected by the intrinsic instability of the μ and τ leptons. We have investigated the likelihood of their formation in astrophysical environments, and the prospects for their observation.

The probability of formation is small, $\sim 10^{-7}$ from photon-photon annihilation or electron-positron annihilation. The probability is small for two reasons: (i) the lifetimes of the μ and τ are intrinsically short (Sec. VB), and thus M and T can only form from the products of pair production processes, such that the pairs immediately recombine, (ii) even then, only those pairs with a total kinetic energy less than the ionization energy can form leptonium, and since pair production usually takes place in high energy processes, these pairs constitute a small fraction of the total. Nevertheless, high energy astrophysical environments are capable of producing copious numbers of μ and τ pairs, and the cross section for radiative recombination dominates that of direct annihilation (Sec. IV). Thus even the small fraction of pairs with energy low enough to form M or T can lead to a significant flux.

The decays of M and T are hastened by the short lifetimes of the μ and τ leptons, which may be one reason why the possibility of astrophysical observations has not

received much attention. Here, we have carefully calculated the probabilities of the various observational signatures. We have calculated the cross sections for recombination onto the nL th level (Sec. IVA), and the resulting branching ratios for Lyman α , Lyman β , Balmer α , Balmer β , two photon annihilation, three photon annihilation, annihilation into e^{\pm} pairs and the decay of either μ or τ . Although the decay of either τ does dominate for T, there is still a small probability for observing recombination lines or two photon annihilation. For M the situation is more hopeful, with significant branching ratios for Lyman α , Balmer α and two photon annihilation.

In Sec. VIII, we made estimates of the fluxes of M and T recombination and annihilation signatures for the cases of blazar jet-cloud interactions, jet-star interactions in misaligned microquasars and within the accretion disks of AGN and microquasars. These were compared to the current detection limits of x-ray and γ -ray observatories. The expected signatures from AGN jet-cloud interactions were all below current detection limits. However, M and T formation within microquasar jet-star interactions, or within the accretion disks of both AGN and microquasars were estimated to yield signatures brighter than the detection limits, with those from microquasars offering the brightest estimates due to their proximity. Actual observations would be further complicated by the intrinsic backgrounds and also the emission from the object in question, which may have other significant line emission (e.g. see Marshall *et al.* [63] for a spectrum of SS 433).

These examples are only illustrative. Other sources may also be significant. For example, 511 keV electron-positron annihilation radiation was recently discovered in terrestrial γ -ray flashes due to lightning strikes [64]. These same flashes could lead to M or T formation, as well as the possibility of observing Ps recombination lines. As a different example we note in passing that the recent detection of an unidentified line at ≈ 3.5 keV in galaxy clusters [18,19] cannot be explained by the T Balmer α line at 3.3 keV, which is ruled out by the constraints on the energy.

In summary, the astrophysics of pair production in any high energy source could lead to possible M and T formation. This paper provides the tools to estimate the fluxes of the M and T recombination and annihilation signatures once the rate of pair production is known.

ACKNOWLEDGMENTS

We thank the referees for useful comments which have improved this paper. We thank M. Voloshin for useful advice regarding the Sommerfeld-Sakharov correction. We thank M. Colless for advice on the nomenclature for leptonium which improved the lucidity of the paper.

**APPENDIX: ENERGY THRESHOLD IN THE
LABORATORY FRAME FOR MUON PAIR
PRODUCTION FROM ELECTRON-POSITRON
ANNIHILATION**

To relate the lab frame energies of the colliding electrons, E_1 and E_2 , to the zero-momentum frame Lorentz factors, γ , of the produced muons, we note that the absolute square of the relativistic four-momentum $p^2 = p^\mu p_\mu$ is invariant. In the lab frame, let the incoming electron be traveling along the x axis in the positive direction, with speed u , and the incoming positron be at an angle θ to the x axis, in the x - y plane, with speed w . The relative speed of the particles in the lab frame is then, $v = u - w \cos \theta$. Therefore in the

lab frame the total relativistic four-momentum of both particles is given by

$$p_{\text{lab}} = \left(\frac{E_1 + E_2}{c}, p_1 + p_2 \cos \theta, p_2 \sin \theta, 0 \right). \quad (\text{A1})$$

In the zero-momentum frame, after the collision, the produced muons have equal and opposite momentum, thus,

$$p_{\text{z.m.}} = \left(\frac{E_3 + E_4}{c}, 0, 0, 0 \right). \quad (\text{A2})$$

Now since p^2 is invariant we have

$$\begin{aligned} p_{\text{lab}}^2 &= p_{\text{z.m.}}^2 \\ \left(\frac{E_1 + E_2}{c} \right)^2 - (p_1 + p_2 \cos \theta)^2 - p_2^2 \sin^2 \theta &= \left(\frac{E_3 + E_4}{c} \right)^2 \\ E_1 E_2 + c^4 (m^2 - 2M^2 \gamma^2) &= \sqrt{E_1^2 - c^4 m^2} \sqrt{E_2^2 - c^4 m^2} \cos \theta. \end{aligned} \quad (\text{A3})$$

Therefore the relative velocity is

$$v = \frac{\sqrt{c^2 E_1^2 - m^2 c^6}}{E_1} - \frac{\sqrt{c^2 E_2^2 - m^2 c^6} \cos \theta}{E_2}. \quad (\text{A4})$$

-
- [1] P. A. M. Dirac, *Proc. Phys. Soc. London Sect. A* **117**, 610 (1928).
[2] P. A. M. Dirac, *Proc. Phys. Soc. London Sect. A* **126**, 360 (1930).
[3] P. A. M. Dirac, *Proc. Phys. Soc. London Sect. A* **133**, 60 (1931).
[4] C. D. Anderson, *Phys. Rev.* **43**, 491 (1933).
[5] S. Mohorovičić, *Astron. Nachr.* **253**, 93 (1934).
[6] J. Pirenne, Ph.D. thesis, University of Paris, 1944.
[7] A. E. Ruark, *Phys. Rev.* **68**, 278 (1945).
[8] A. Alichanian and T. Asatiani, *J. Phys. U.S.S.R.* **9**, 56 (1945).
[9] J. A. Wheeler, *Ann. N.Y. Acad. Sci.* **48**, 219 (1946).
[10] J. E. McClintock, *Astrophys. J.* **282**, 291 (1984).
[11] V. V. Burdyuzha and V. L. Kauts, *Astrophys. Space Sci.* **258**, 329 (1997).
[12] S. C. Ellis and J. Bland-Hawthorn, *Astrophys. J.* **707**, 457 (2009).
[13] M. Leventhal, C. J. MacCallum, and P. D. Stang, *Astrophys. J.* **225**, L11 (1978).
[14] N. Prantzios, C. Boehm, A. M. Bykov, R. Diehl, K. Ferrière, N. Guessoum, P. Jean, J. Knoedlseder, A. Marcowith, I. V. Moskalenko *et al.*, *Rev. Mod. Phys.* **83**, 1001 (2011).
[15] C. Avilez, E. Ley-Koo, and M. Moreno, *Phys. Rev. D* **19**, 2214 (1979).
[16] H. I. Ewen and E. M. Purcell, *Nature (London)* **168**, 356 (1951).
[17] C. A. Muller and J. A. Oort, *Nature (London)* **168**, 357 (1951).
[18] A. Boyarsky, O. Ruchayskiy, D. Iakubovskiy, and J. Franse, *Phys. Rev. Lett.* **113**, 251301 (2014).
[19] E. Bulbul, M. Markevitch, A. Foster, R. K. Smith, M. Loewenstein, and S. W. Randall, *Astrophys. J.* **789**, 13 (2014).
[20] S. J. Brodsky and R. F. Lebed, *Phys. Rev. Lett.* **102**, 213401 (2009).
[21] R. J. Gould, *Astrophys. J.* **344**, 232 (1989).
[22] P. Wallyn, W. A. Mahoney, P. Durouchoux, and C. Chapuis, *Astrophys. J.* **465**, 473 (1996).
[23] P. Jean, J. Knödlseder, W. Gillard, N. Guessoum, K. Ferrière, A. Marcowith, V. Lonjou, and J. P. Roques, *Astron. Astrophys.* **445**, 579 (2006).
[24] The nomenclature for such systems is somewhat confusing. A bound state of a particle and its antiparticle is called an onium, however the name muonium is already given to the combination of an antimuon with an electron to form a

hydrogenlike atom, and by analogy tauonium refers to an antitauon and an electron. Therefore the systems $\mu^- - \mu^+$ and $\tau^- - \tau^+$ are usually referred to as *true* muonium and *true* tauonium, however to avoid confusion, and for brevity, we prefer to use the symbols M and T.

- [25] R. W. Bussard, R. Ramaty, and R. J. Drachman, *Astrophys. J.* **228**, 928 (1979).
- [26] N. Guessoum, P. Jean, and W. Gillard, *Astron. Astrophys.* **436**, 171 (2005).
- [27] R. J. Gould and G. P. Schröder, *Phys. Rev.* **155**, 1404 (1967).
- [28] S. Bonometto and M. J. Rees, *Mon. Not. R. Astron. Soc.* **152**, 21 (1971).
- [29] F. A. Agaronyan, A. M. Atoyan, and A. M. Nagapetyan, *Astrophysics (Engl. Transl.)* **19**, 187 (1983).
- [30] P. S. Coppi and R. D. Blandford, *Mon. Not. R. Astron. Soc.* **245**, 453 (1990).
- [31] M. Böttcher and R. Schlickeiser, *Astron. Astrophys.* **325**, 866 (1997).
- [32] J. M. Jauch and F. Rohrlich, *Theory of Photons and Electrons* (Addison-Wesley, Reading, MA, 1955).
- [33] A. D. Sakharov, *Zh. Eksp. Teor. Fiz.* **18**, 631 (1948).
- [34] A. D. Sakharov, *Sov. Phys. Usp.* **34**, 375 (1991).
- [35] M. B. Voloshin, *Phys. Lett. B* **556**, 153 (2003).
- [36] M. L. Perl, *Rep. Prog. Phys.* **55**, 653 (1992).
- [37] R. Gould, *Ann. Phys. (N.Y.)* **69**, 321 (1972).
- [38] C. N. Yang, *Phys. Rev.* **77**, 242 (1950).
- [39] L. Wolfenstein and D. G. Ravenhall, *Phys. Rev.* **88**, 279 (1952).
- [40] P. A. M. Dirac, *Proc. Cambridge Philos. Soc.* **26**, 361 (1930).
- [41] A. Ore and J. L. Powell, *Phys. Rev.* **75**, 1696 (1949).
- [42] S. Berko and H. N. Pendleton, *Annu. Rev. Nucl. Part. Sci.* **30**, 543 (1980).
- [43] L. C. Green, P. P. Rush, and C. D. Chandler, *Astrophys. J. Suppl. Ser.* **3**, 37 (1957).
- [44] R. M. Pengelly, *Mon. Not. R. Astron. Soc.* **127**, 145 (1964).
- [45] M. Brocklehurst, *Mon. Not. R. Astron. Soc.* **153**, 471 (1971).
- [46] W. Gordon, *Ann. Phys. (Berlin)* **394**, 1031 (1929).
- [47] D. E. Osterbrock and G. J. Ferland, *Astrophysics of Gaseous Nebulae and Active Galactic Nuclei* (University Science Books, Herndon, VA, 2006).
- [48] M. J. Seaton, *Mon. Not. R. Astron. Soc.* **119**, 90 (1959).
- [49] G. Hasinger, B. Altieri, M. Arnaud, X. Barcons, J. Bergeron, H. Brunner, M. Dadina, K. Dennerl, P. Ferrando, A. Finoguenov *et al.*, *Astron. Astrophys.* **365**, L45 (2001).
- [50] A. Celotti and A. C. Fabian, *Mon. Not. R. Astron. Soc.* **264**, 228 (1993).
- [51] C. S. Reynolds, A. C. Fabian, A. Celotti, and M. J. Rees, *Mon. Not. R. Astron. Soc.* **283**, 873 (1996).
- [52] J. F. C. Wardle, D. C. Homan, R. Ojha, and D. H. Roberts, *Nature (London)* **395**, 457 (1998).
- [53] K. Hirotani, *Astrophys. J.* **619**, 73 (2005).
- [54] R. D. Blandford and A. Levinson, *Astrophys. J.* **441**, 79 (1995).
- [55] M. C. Begelman, R. D. Blandford, and M. J. Rees, *Rev. Mod. Phys.* **56**, 255 (1984).
- [56] M. Boettcher and R. Schlickeiser, *Astron. Astrophys.* **306**, 86 (1996).
- [57] A. P. Marscher, S. G. Jorstad, J. L. Gómez, I. M. McHardy, T. P. Krichbaum, and I. Agudo, *Astrophys. J.* **665**, 232 (2007).
- [58] J.-L. Gómez, A. P. Marscher, A. Alberdi, S. G. Jorstad, and C. García-Miró, *Science* **289**, 2317 (2000).
- [59] N. Guessoum, P. Jean, and N. Prantzos, *Astron. Astrophys.* **457**, 753 (2006).
- [60] A. P. Marscher, *Astrophys. J.* **264**, 296 (1983).
- [61] G. Ghisellini, P. Padovani, A. Celotti, and L. Maraschi, *Astrophys. J.* **407**, 65 (1993).
- [62] A. M. Beloborodov, *Mon. Not. R. Astron. Soc.* **305**, 181 (1999).
- [63] H. L. Marshall, C. R. Canizares, and N. S. Schulz, *Astrophys. J.* **564**, 941 (2002).
- [64] M. S. Briggs, V. Connaughton, C. Wilson-Hodge, R. D. Preece, G. J. Fishman, R. M. Kippen, P. N. Bhat, W. S. Paciesas, V. L. Chaplin, C. A. Meegan *et al.*, *Geophys. Res. Lett.* **38**, L02808 (2011).